WIRTSCHAFTS UNIVERSITÄT WIEN VIENNA UNIVERSITY OF ECONOMICS AND BUSINESS

EFMD EQUIS ACCREDITED

ePub^{WU} Institutional Repository

Manfred M. Fischer and Florian Huber and Michael Pfarrhofer

The regional transmission of uncertainty shocks on income inequality in the United States

Paper

Original Citation:
Fischer, Manfred M. and Huber, Florian and Pfarrhofer, Michael (2019) The regional transmission of uncertainty shocks on income inequality in the United States. *Working Papers in Regional Science*, 2019/01. WU Vienna University of Economics and Business, Vienna.

This version is available at: http://epub.wu.ac.at/6774/
Available in ePub^{WU}: January 2019

ePub^{WU}, the institutional repository of the WU Vienna University of Economics and Business, is provided by the University Library and the IT-Services. The aim is to enable open access to the scholarly output of the WU.

http://epub.wu.ac.at/

The regional transmission of uncertainty shocks on income inequality in the United States

MANFRED M. FISCHER[1], FLORIAN HUBER[2*] and MICHAEL PFARRHOFER[1,2]

[1]*Vienna University of Economics and Business*

[2]*Salzburg Centre of European Union Studies, University of Salzburg*

This paper explores the relationship between household income inequality and macroeconomic uncertainty in the United States. Using a novel large-scale macroeconometric model, we shed light on regional disparities of inequality responses to a national uncertainty shock. The results suggest that income inequality decreases in most states, with a pronounced degree of heterogeneity in terms of the dynamic responses. By contrast, some few states, mostly located in the Midwest, display increasing levels of income inequality over time. Forecast error variance and historical decompositions highlight the importance of uncertainty shocks in explaining income inequality in most regions considered. Finally, we explain differences in the responses of income inequality by means of a simple regression analysis. These regressions reveal that the income composition as well as labor market fundamentals determine the directional pattern of the dynamic responses.

JEL CODES: C11, C30, E3, D31

KEYWORDS: Income distribution, US states, macroeconomic volatility, global vector autoregressive model

January 10, 2019

*Corresponding author: Florian Huber. Salzburg Centre of European Union Studies, University of Salzburg. Address: Mönchsberg 2a, 5020 Salzburg, Austria. Email: florian.huber@sbg.ac.at. The authors gratefully acknowledge financial support from the Austrian National Bank, Jubilaeumsfond grant no. 17650.

1. INTRODUCTION

This paper explores the nexus between uncertainty shocks and income inequality in the US states. Uncertainty shocks impact the wider economy through a range of various channels. For instance, if uncertainty increases, companies change their investment and hiring behavior, leading to a decline in real activity. This drop in output may impact aggregate demand which, in turn, affects prices. Movements in quantities related to these channels are typically perceived as important determinants of income inequality (Piketty and Saez, 2003; Roine et al., 2009; Coibion et al., 2017). In this contribution, we propose a large-scale dynamic model to analyze how movements in uncertainty impact household income inequality within US states. Our model enables us to capture dynamics between national macroeconomic fundamentals and state-level variables related to the distribution of income, a feature that is novel to the literature.

The recent literature on uncertainty shocks (see, inter alia, Bloom, 2009; Caggiano et al., 2014; Jurado et al., 2015; Caldara et al., 2016; Baker et al., 2016; Basu and Bundick, 2017; Mumtaz and Theodoridis, 2018; Carriero et al., 2018) increasingly discriminates between different types of uncertainty. In his seminal contribution, Bloom (2009), for instance, uses the volatility index of the Chicago Board Options Exchange as an observed measure of uncertainty that is closely related to financial market uncertainty. As opposed to uncertainty arising from financial markets, real macroeconomic uncertainty is associated with unexpected fluctuations in output or prices. Other studies highlight that uncertainty might also be linked to unexpected actions of policy makers in central banks and the government (Baker et al., 2016). All types of uncertainty have in common, however, that they are generally perceived to be detrimental for economic performance, at least in the short-run. For instance, the latest global financial crisis can be viewed as a US-based uncertainty shock that ultimately engulfed the world economy and led to a sharp decline in economic activity.

During economic downturns, income inequality has been found to decrease (see, for instance, Heathcote et al., 2010; Petev et al., 2011; Meyer and Sullivan, 2013; Mumtaz and Theophilopoulou, 2017; Theophilopoulou, 2018). This finding, however, depends on the composition of income. A potential explanation might be that capital owners are more exposed to adverse business cycle movements, which are often accompanied by sharp declines in corporate profits and stock prices. By contrast, if the income share of capital is comparatively low in a given economy, inequality could also increase during recessions. This is due to the notion that less skilled workers are typically more vulnerable to movements in labor markets and technological change. Understanding the mechanisms that give rise to changes in income inequality proves to be important for policy makers in governmental institutions and central banks alike, since several studies highlight the relation between household income inequality and the emergence of crises (see, for instance, Stiglitz, 2012; van Treeck, 2014, and the references therein).

The empirical literature dealing with the dynamic relationship between uncertainty and income inequality is non-existent or sparse, at best (see Theophilopoulou, 2018, for a notable exception). The present contribution attempts to fill this gap by considering data on unemployment, real income, employment, and a survey-based measure of income inequality for all US states, including the District of Columbia. State-level information is complemented by a set of national macroeconomic aggregates that serve as common driving factors of state business cycles. Taking such a regional perspective allows a detailed investigation on whether national uncertainty shocks yield asymmetric responses across space while the inclusion of covariates at the national level provides the possibility to inspect the transmission mechanisms of uncertainty shocks on income inequality in more detail.

For addressing the research question, we suggest a parsimonious framework closely related to the global vector autoregressive (GVAR) model proposed in Pesaran et al. (2004). The model approach differs along several important dimensions. First, inspired by the panel data literature, state-specific regression coefficients are assumed to arise from an underlying common distribution. This improves estimation accuracy while maintaining sufficient flexibility to allow for differing features across states. Second, one key assumption of the model is that contemporaneous relations among the states and variables are driven by a small number of latent factors. This reduces the amount of free parameters to be estimated significantly. Third, we assume that all shocks to the system are heteroscedastic and follow a flexible stochastic volatility specification. Finally, structural identification of the uncertainty shock is achieved by using the measure proposed in Baker et al. (2016) that approximates general macroeconomic policy uncertainty.

The empirical findings reveal that uncertainty shocks lead to heterogeneous responses across space, with most US states displaying decreasing levels of income inequality while some few, predominantly located in the Midwest, exhibit increasing levels of income dispersion. Forecast error variance and historical decompositions identify uncertainty to be an important driver of variation in income inequality, especially for certain regions and during selected time periods. Explaining the differences in income inequality reactions by means of a simple regression exercise shows that differences across states may be explained by the composition of income and labor market fundamentals.

The remainder of the paper is structured as follows. Section 2 presents the econometric framework adopted while Section 3 provides a brief summary of the dataset used and specifics about model specification and structural identification. Section 4 describes the empirical findings based on structural impulse responses, forecast error and historical decompositions, combined with a brief discussion on what determines differences in inequality responses. The last section summarizes and concludes the paper.

2. ECONOMETRIC FRAMEWORK

In this section, we describe the empirical framework. Section 2.1 presents the global vector autoregressive model for state-specific quantities augmented with variables at the national level. A flexible specification for modeling co-movement and time-variation in the variance-covariance matrix is provided. Section 2.2 discusses prior selection required for Bayesian estimation of the model.

2.1. *The model*

To measure the impact of uncertainty on income inequality across US states, a suitable econometric framework is necessary. Inclusion of the $N = 51$ US states alongside a moderate number of state-specific endogenous variables calls for a modeling approach that adequately captures dynamic relations in the data. We follow Pesaran et al. (2004) and propose a variant of the GVAR model involving N small-scale state-specific models. These state models feature domestic variables, indexed by $i = 1, \dots, N$ and collected in the k-dimensional vector $\{\boldsymbol{y}_{it}\}_{t=1}^{T}$, besides cross-sectional averages of foreign variables specific to each state,[1] collected in the k-dimensional vector

$$\boldsymbol{y}_{it}^{*} = \sum_{j=1}^{N} w_{ij} \boldsymbol{y}_{jt}, \tag{1}$$

where the weights w_{ij} $(i, j = 1, \ldots, N)$ represent the connectivity relationships between the N states. By convention, $w_{ii} = 0, w_{ij} \geq 0$ and $\sum_{j=1}^{N} w_{ij} = 1$ for all i, j. The higher the connectedness is between states i and j (that is, the larger w_{ij} is), the more state i is exposed to externalities arising in state j.

The state economies may then be modeled as a vector autoregression (VAR) augmented by a vector of lagged foreign variables, and a set of national macroeconomic aggregates that are assumed to be important determinants of state business cycle dynamics,

$$\boldsymbol{y}_{it} = \boldsymbol{\theta}_i + \sum_{p=1}^{P} \boldsymbol{A}_{ip} \boldsymbol{y}_{it-p} + \sum_{q=1}^{Q} \boldsymbol{B}_{iq} \boldsymbol{y}_{it-q}^{*} + \boldsymbol{C}_i \boldsymbol{z}_{t-1} + \boldsymbol{\epsilon}_{it}, \quad \boldsymbol{\epsilon}_{it} \sim \mathcal{N}(\boldsymbol{0}, \boldsymbol{\Sigma}_{it}). \tag{2}$$

Hereby, $\boldsymbol{\theta}_i$ is a k-dimensional intercept vector, while $\boldsymbol{A}_{ip}$ $(p = 1, \ldots, P)$ and $\boldsymbol{B}_{iq}$ $(q = 1, \ldots, Q)$ are $k \times k$ matrices of unknown parameters, respectively. $\boldsymbol{C}_i$ is a $k \times \ell$ matrix of regression coefficients associated with ℓ national macroeconomic aggregates collected in $\boldsymbol{z}_t$. The error term $\boldsymbol{\epsilon}_{it}$ follows a zero mean Gaussian distribution with a time-varying variance-covariance matrix $\boldsymbol{\Sigma}_{it}$.

The national aggregates in $\boldsymbol{z}_t$ follow a VAR process,

$$\boldsymbol{z}_t = \sum_{p=1}^{P} \boldsymbol{D}_p \boldsymbol{z}_{t-p} + \sum_{q=1}^{Q} \boldsymbol{S}_q \boldsymbol{z}_{t-q}^{*} + \boldsymbol{u}_t, \quad \boldsymbol{u}_t \sim \mathcal{N}(\boldsymbol{0}, \boldsymbol{\Xi}_t), \tag{3}$$

with $\boldsymbol{D}_p$ $(p = 1, \ldots, P)$ and $\boldsymbol{S}_q$ $(q = 1, \ldots, Q)$ denoting $\ell \times \ell$ and $\ell \times k$ coefficient matrices. To establish dependencies between the national aggregates and the state-specific variables, Eq. (3) also features averages of the k state-level quantities over N states, denoted by $z_t^* = (z_{1t}^*, \ldots, z_{kt}^*)'$. Again, we assume the error term $\boldsymbol{u}_t$ to follow a Gaussian distribution centered on zero with time-varying variance-covariance matrix $\boldsymbol{\Xi}_t$.

To capture contemporaneous relations among the elements in $\boldsymbol{y}_t = (\boldsymbol{y}_{1t}', \ldots, \boldsymbol{y}_{Nt}')'$ and $\boldsymbol{z}_t$, we assume that the shock vector $\boldsymbol{\varepsilon}_t = (\boldsymbol{u}_t', \boldsymbol{\epsilon}_{1t}', \ldots, \boldsymbol{\epsilon}_{Nt}')'$ of size $L = kN + \ell$ has a factor stochastic volatility structure (Aguilar and West, 2000),[2] that is,

$$\boldsymbol{\varepsilon}_t = \boldsymbol{\Lambda} \boldsymbol{f}_t + \boldsymbol{\eta}_t. \tag{4}$$

$\boldsymbol{f}_t \sim \mathcal{N}(\boldsymbol{0}, \boldsymbol{H}_t)$ represents a set of $F (\ll L)$ common static factors with zero mean, $\boldsymbol{\Lambda}$ is an $L \times F$ matrix of factor loadings, and $\boldsymbol{\eta}_t \sim \mathcal{N}(\boldsymbol{0}, \boldsymbol{\Omega}_t)$ denotes an L-dimensional idiosyncratic noise vector. The variance-covariance matrices $\boldsymbol{H}_t = \text{diag}[\exp(h_{1t}), \ldots, \exp(h_{Ft})]$ and $\boldsymbol{\Omega}_t = \text{diag}[\exp(\omega_{1t}), \ldots, \exp(\omega_{Lt})]$ are diagonal matrices, implying that any co-movement across the elements in $\boldsymbol{\varepsilon}_t$ stems from the common factors. We control for heteroscedasticity of the shocks by assuming that the logarithm of the main diagonal elements follows an autoregressive process of order one. This setup implies that $\text{Var}(\boldsymbol{\varepsilon}_t) = \boldsymbol{\Lambda} \boldsymbol{H}_t \boldsymbol{\Lambda}' + \boldsymbol{\Omega}_t := \boldsymbol{\Theta}_t$.

[1]Domestic in the sense of within and foreign in the sense of outside the state concerned.

[2]See Huber (2016) for a variant of the GVAR model that features a factor stochastic volatility specification on the shocks.

Following Aguilar and West (2000), the logarithms of the main diagonal elements of $\boldsymbol{H}_t$ and $\boldsymbol{\Omega}_t$ are assumed to evolve according to independent first-order autoregressive processes,

$$h_{jt} = \phi_{hj} + \rho_{hj}(h_{jt-1} - \phi_{hj}) + \sigma_{hj}\xi_{hj,t} \qquad \text{for} \quad j = 1, \ldots, F, \tag{5}$$
$$\omega_{jt} = \phi_{\omega j} + \rho_{\omega j}(\omega_{jt-1} - \phi_{\omega j}) + \sigma_{\omega j}\xi_{\omega j,t} \qquad \text{for} \quad j = 1, \ldots, L, \tag{6}$$

and using $s \in \{h, \omega\}$, we denote the unconditional mean of the log-volatility by ϕ_{sj}, the autoregressive parameter by ρ_{sj}, and σ^2_{sj} is the innovation variance of the processes. The serially uncorrelated white noise shocks $\xi_{sj,t} \sim \mathcal{N}(0, 1)$ are standard normally distributed.

Since unrestricted estimation of the model typically translates into overfitting issues, additional structure on the coefficients of the model in Eq. (2) is imposed. In what follows, we assume that the $M = k(1 + Pk + Qk + \ell)$ vectorized regression coefficients $\boldsymbol{\beta}_i = \text{vec}[(\boldsymbol{\theta}_i, \boldsymbol{A}_{i1}, \ldots, \boldsymbol{A}_{iP}, \boldsymbol{B}_{i1}, \ldots, \boldsymbol{B}_{iQ}, \boldsymbol{C}_i)']$ for state $i = 1, \ldots, N$ arise from a common distribution,

$$\boldsymbol{\beta}_i \sim \mathcal{N}(\boldsymbol{\mu}, \boldsymbol{V}), \tag{7}$$

where $\boldsymbol{\mu}$ denotes a common mean and $\boldsymbol{V} = \text{diag}(v_1, \ldots, v_M)$ a variance-covariance matrix. Notice that v_j $(j = 1, \ldots, M)$ provides a natural measure of similarity between the jth element in $\boldsymbol{\beta}_i$ $(i = 1, \ldots, N)$ across states, controlling the magnitude of potential deviations from μ_j, the jth element $\boldsymbol{\mu}$. The presence of the common distribution implies that our framework is a hierarchical model that is related to random coefficient models in microeconometrics (Verbeke and Lesaffre, 1996; Allenby et al., 1998) and the panel VAR specification outlined in Jarociński (2010).

2.2. *Bayesian estimation*

Estimating the model requires Bayesian methods that involve choosing adequate prior distributions for the parameters.[3] Notice that in Section 2.1, the vectorized VAR coefficients $\boldsymbol{\beta}_i$ arise from a common distribution. Equation (7) can be interpreted as a prior distribution on $\boldsymbol{\beta}_i$ with mean $\boldsymbol{\mu}$ and diagonal variance-covariance matrix $\boldsymbol{V}$. On $\boldsymbol{\mu}$, we use a normally distributed prior,

$$\boldsymbol{\mu} \sim \mathcal{N}(\boldsymbol{0}, \boldsymbol{V}_0), \tag{8}$$

and set $\boldsymbol{V}_0 = 10 \times \boldsymbol{I}$.

For the main diagonal elements of $\boldsymbol{V}$, v_j $(j = 1, \ldots, M)$, we adopt independent inverted Gamma priors,

$$v_j \sim \mathcal{G}^{-1}(d_0, d_1), \tag{9}$$

where the prior hyperparameters $d_0 = d_1 = 0.01$ are set to be only weakly informative.

The coefficient matrices $\boldsymbol{D}_p$ and $\boldsymbol{S}_q$ for the national quantities are assigned a Gaussian prior with the mean vector centered on zero with variance ten. This choice introduces relatively little prior information on these coefficients.

[3]For recent Bayesian expositions to GVAR models, see Crespo Cuaresma et al. (2016); Feldkircher and Huber (2016), and Huber et al. (2017).

For the factor specification in the reduced form errors of the model, we employ the following prior setup. The elements λ_{ij} of the matrix of factor loadings $\mathbf{\Lambda}$ for $i = 1, \ldots, L$ and $j = 1, \ldots, F$ are assigned a normally distributed prior, that is, $\lambda_{ij} \sim \mathcal{N}(0, 0.1)$. The prior specification on the log-volatility equations closely follows Kastner and Frühwirth-Schnatter (2014), with a normally distributed prior on $\phi_{sj} \sim \mathcal{N}(0, 10^2)$, a Gamma prior on $\sigma^2_{sj} \sim \mathcal{G}(1/2, 1/2)$ and a Beta prior on the transformed persistence parameter $(\rho_{sj} + 1)/2 \sim \mathcal{B}(25, 5)$.

After specifying suitable prior distributions, estimation is carried out using a Markov chain Monte Carlo (MCMC) algorithm. This algorithm is based on drawing from well-known conditional posterior distributions until convergence is achieved. In this study, we run our algorithm 50,000 times where we discard the first 25,000 draws as burn-in. Inference presented throughout this paper is based on considering every fifth draw from the stored posterior distributions. Appendix A provides details on the MCMC algorithm.

3. DATA, MODEL SPECIFICATION, AND STRUCTURAL IDENTIFICATION

This section establishes the state-level measure of household income inequality and provides a brief summary of the dataset in Section 3.1, while outlining specifics about model specification and structural identification in Section 3.2.

3.1. *Data*

To estimate our model, we use a panel of quarterly data starting in 1985:Q1 to 2017:Q1. The inequality measure for all the states is constructed using data from the Annual Social and Economic Supplement of the Current Population Survey (CPS, Flood et al., 2017). Income is defined as equivalized household income on the square root scale (see OECD, 2011). Accordingly, we divide the sum of all individual incomes in a given household by the square root of the number of its members to obtain a measure of income that is comparable across different household sizes. The measure on household income includes all types of total pre-tax income or losses. We take the well-known Gini coefficient as our scalar measure of household income inequality (Cowell and Flachaire, 2015).[4] To produce unbiased household-level statistics per year and state, we rely on the complex stratified sampling scheme of the CPS. Here, the last available census resident population characteristics are taken as a reference for creating representative household weights to achieve accurate estimates for the entire population based on the information contained in the survey sample.[5] This annual measure of household income inequality is interpolated to the quarterly frequency using splines.

The remaining three state-level quantities in $\boldsymbol{y}_{it}$ are obtained from the Federal Reserve Bank of St. Louis database. More specifically, we make use of data for unemployment, employment, and real per capita total personal income. These quantities allow for measuring the consequences of increases in

[4]The employed definition of household income results in a small number of negative incomes (around 0.74 percent of the full sample). For the baseline specification, we include all available households. Calculating the Gini coefficient after dropping negative incomes as well as setting negative incomes to zero yields similar results, with a correlation > 0.99 to the Gini coefficient based on all households for all states.

[5]Calculations are carried out using the R software packages provided by Lumley (2004, 2018) and Pessoa et al. (2018).

uncertainty on the real side of the economy, putting special emphasis on labor market effects as well as income reactions. For the empirical specification, we thus have a set of $k = 4$ quantities in $\boldsymbol{y}_{it}$ (household income inequality, total personal income, unemployment, and employment).

Four national macroeconomic quantities are included in $\boldsymbol{z}_t$, namely the consumer price index (CPI), taken from the dataset presented in McCracken and Ng (2016) and consequently transformed into quarterly frequency, US gross domestic product (GDP) obtained from the National Income and Product Accounts provided by the Bureau of Economic Analysis,[6] the one-year treasury rate and national macroeconomic uncertainty.

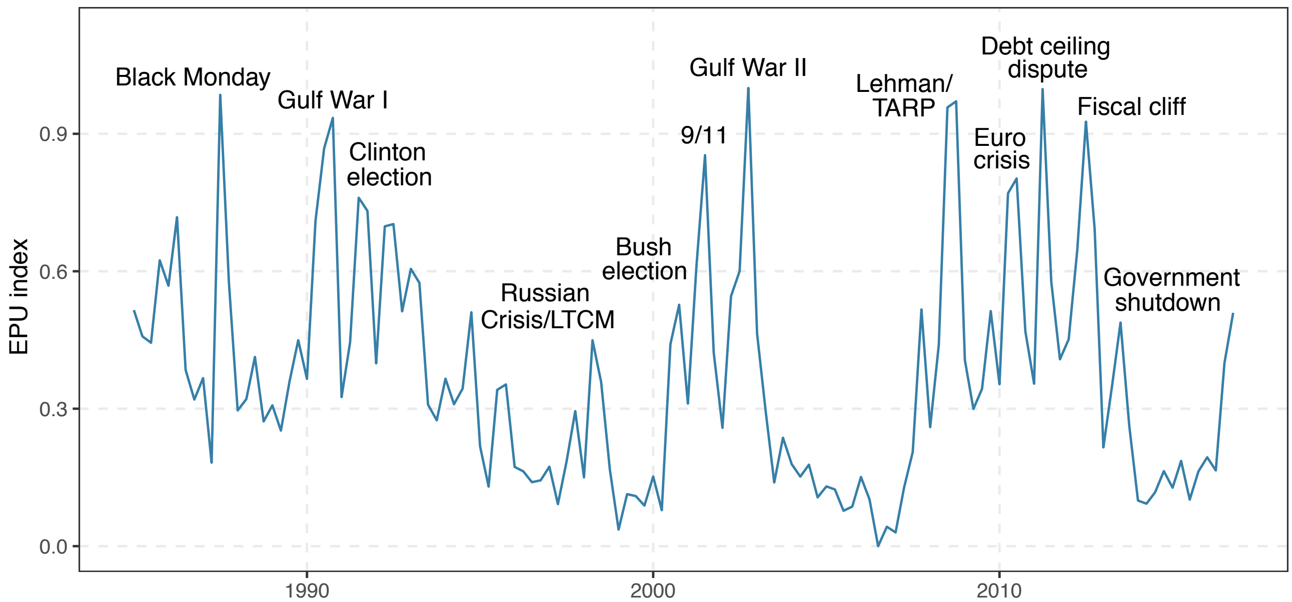

Fig. 1: Economic policy uncertainty and related events.
Notes: The solid blue line is the economic policy uncertainty (EPU) index by Baker et al. (2016) normalized to the unit interval. LTCM refers to the collapse of Long-Term Capital Management, while TARP denotes the Troubled Asset Relief Program by the United States government.

To capture national economic uncertainty, we rely on the overall economic policy uncertainty (EPU) index provided by Baker et al. (2016). This index is comprised of three weighted components. The first component is based on screening ten large US newspapers for economic and policy uncertainty related keywords (weighted by 1/2) while the second component reflects temporary federal tax code provisions (receiving a weight of 1/6). The last component uses the Federal Reserve Bank of Philadelphia's Survey of Professional Forecasters to capture expectations on the consumer price index and purchases of goods and services by federal, state and local governments (each weighted by 1/6). Figure 1 provides some intuition of the evolution of the uncertainty index over time, with peaks during events commonly associated with high levels of economic and political uncertainty (for instance, the index reaches historically high levels during the stock market crash in 1987, both Gulf Wars, the 9/11 terrorist attacks, and the Lehman bankruptcy) while being low during periods of relative tranquility.

[6]Available for download at `bea.gov/iTable/index_nipa.cfm`.

Finally, it should be noted that the uncertainty index is logarithmically transformed, while the one-year treasury rate is in levels. For GDP and the CPI, we take log-differences. State-level quantities are adjusted as follows. We deseasonalize the unemployment rates and include them in levels. The Gini coefficients are logarithmically transformed, and employment and total personal income enter the model in first log-differences.

3.2. *Model specification and structural identification*

For the empirical application the lag length equals $P = Q = 1$. Based on the deviance information criterion (DIC, see Spiegelhalter et al., 2002) , we opt for $F = 2$ latent factors and select the appropriate weights w_{ij}. Specifically, the model is computed over a grid of alternative weighting schemes based on k-nearest neighbors (for $k = 3, \ldots, 9$), inverse distances and equal distances between i and j, respectively.[7] For each of these models, the DIC is calculated and the specification that yields the smallest DIC (in our case five nearest neighbors) is chosen.

Before proceeding, a brief word on structural identification is in order. In the present paper, we follow Baker et al. (2016) and include the economic policy uncertainty (EPU) index as the first variable in z_t. Identification of the model is then achieved by using a simple Cholesky decomposition of the variance-covariance matrix. This implies that all quantities in the system react to movements in uncertainty contemporaneously, while for other shocks in the system we introduce a causal ordering. This specification also mirrors the approach used in Bloom (2009) who adopts a stock market volatility index as a proxy for uncertainty.

4. EMPIRICAL RESULTS

The following section presents the main empirical findings of the study. Section 4.1 displays the responses of the national and subnational macroeconomic quantities with respect to movements in uncertainty while Section 4.2 shows the dynamic responses of state-level inequality to national uncertainty shocks. To assess the quantitative importance of uncertainty shocks in shaping the income distribution, we compute forecast error variance and historical decompositions in Section 4.3. The last subsection aims at explaining the differences in the dynamic responses of income inequality across space.

4.1. *Dynamic responses of national and state-level macroeconomic quantities*

We start our discussion by considering the responses of the national macroeconomic aggregates. The impulse responses of the aggregates at the national level serve to assess whether our high-dimensional model approach yields responses consistent with established findings in the literature and, moreover, to shed some light on potential linkages between the national and state-level quantities. Figure 2 presents the endogenous responses to a positive one standard error shock to the EPU index that amounts to an immediate reaction of around 30 percent. All plots include the median response (in blue) for 20 quarters alongside the 68 percentiles of the posterior distribution (in light blue). The red line denotes the zero line.

[7]For a survey of alternative weighting schemes, see Fischer and Wang (2011, pp. 19–26).

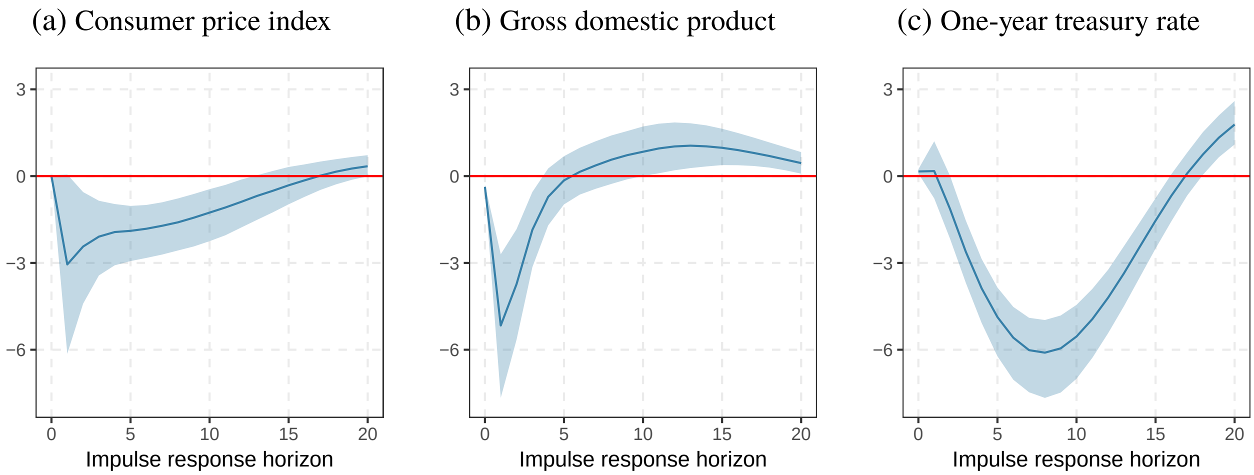

Fig. 2: Impulse responses of national US quantities following a national uncertainty shock.
Notes: The solid blue line is the median response, the shaded blue area represents the 16th and 84th percentiles. The red line indicates the zero line. Results are based on 5,000 posterior draws. Sample period: 1985:Q1 – 2017:Q1. Front axis: quarters after impact.

Starting with price reactions, Fig. 2(a) indicates that inflation significantly decreases by approximately three percentage points after around one quarter, remaining negative for about three years with a tendency to increase. This reaction can be traced back to strong declines in consumption which, in turn, lowers demand for goods, and firms accordingly adjust prices. This mechanism is commonly referred to as the aggregate demand channel. By contrast, there is only little evidence in favor of the upward pricing bias channel (see, e.g., Fernández-Villaverde et al., 2011) that states that firms increase prices to maximize profits in the aftermath of an uncertainty shock.

Next, we consider the reactions of output in Fig. 2(b), measured in terms of GDP. The figure reveals that GDP growth strongly declines in the short run, peaking after approximately one quarter. Output reactions, however, turn insignificant after one year, and there exists some evidence of an overshoot in real activity after roughly three years. This rebound in real activity can be attributed to the fact that companies, when faced with elevated levels of macroeconomic uncertainty, tend to postpone investments in the short run. However, if uncertainty dissipates, firms start investing again and this boosts output through increasing investment. Recent literature (Jurado et al., 2015; Carriero et al., 2018; Mumtaz and Theophilopoulou, 2017) finds only little evidence of a real activity overshoot but it is worth noting that these studies estimate the uncertainty factor alongside the remaining model parameters, while studies reporting some evidence for a rebound in output rely, as we do, on observed proxies of uncertainty (see, e.g., Bloom, 2009).

The final national macroeconomic quantity is the one-year treasury rate, shown in Fig. 2(c).[8] Consistent with Bloom (2009), increases in uncertainty translate into lower interest rates. Notice that, without

[8]Instead of using the Federal Funds rate as a measure of the monetary policy stance, we opt for interest rate securities with a slightly longer maturity due to the fact that our dataset covers the period of the zero lower bound on interest rates. Using longer-run interest rates thus provides a broader picture of the monetary policy stance, effectively covering actions related to forward guidance and unconventional monetary policy (Gertler and Karadi, 2015).

imposing zero impact restrictions, this decrease tends to materialize after around one quarter following the uncertainty shock hitting our model economy. This implies that the Federal Reserve counteracts the detrimental impact of uncertainty shocks on output and prices by lowering key interest rates, but with at least one quarter delay. At the peak (about two years), the decline in interest rates reaches roughly six percentage points.

While Fig. 2 provides a picture on how macroeconomic fundamentals react to changes in uncertainty at the national level, Figs. (3)–(5) asses how a national uncertainty shock impacts unemployment, employment, and income at the regional level. Since presenting the responses of all states is infeasible, we present census region-level rather than state-level impulse responses, using weighted averages reflecting the relative sizes of the economies (measured in terms of gross state product).[9]

Figure 3 indicates that unemployment increases in a hump-shaped manner, peaking after about a year. The increase in unemployment ranges from 2.5 to 3.8 percentage points in the Midwest and West, respectively. These reactions are consistent with Leduc and Liu (2016), who report increasing unemployment to uncertainty shocks. It is noteworthy that the dynamic responses of unemployment turn negative after around 3.5 years, in agreement with the decline in real GDP at the national level. This finding appears to confirm the hypothesis that when faced with increased levels of uncertainty, firms alter their behavior and postpone hiring new employees until the economic outlook becomes more secure. Figure 3, moreover, suggests that cross-regional differences in unemployment responses are small.

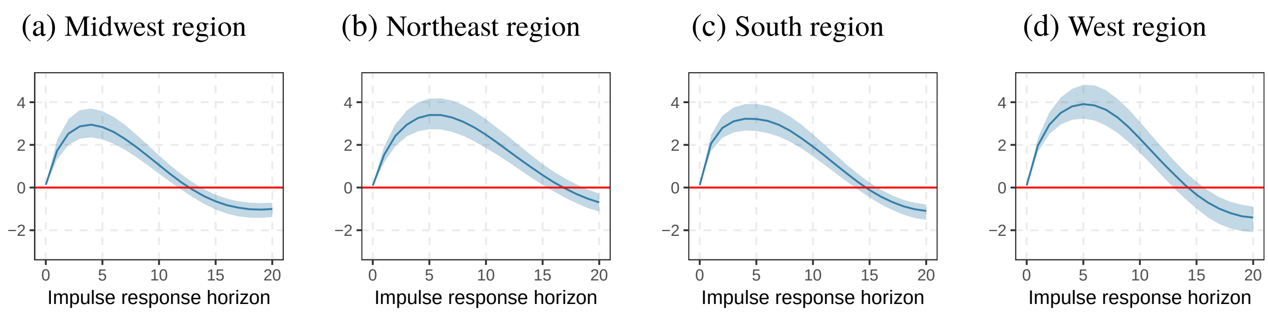

Fig. 3: Impulse response functions of unemployment in US states following a national uncertainty shock. *Notes*: The solid blue line is the median response, the shaded blue area represents the 16th and 84th percentiles. The red line indicates the zero line. Results are based on 5,000 posterior draws. Sample period: 1985:Q1 – 2017:Q1. Front axis: quarters after impact.

Employment responses (see Fig. 4) tend to be inversely related to those reported for unemployment. Instead of being hump-shaped, the impulse responses of employment indicate a pronounced immediate reaction, yielding decreases in employment by around five percent throughout the regions. These labor market responses, however, become smaller over the first two years of the impulse response horizon. After approximately two years, companies start hiring again, and employment subsequently increases. Only little cross-regional variation is visible, both in the size and shape of the dynamic responses between the regional aggregates under scrutiny.

Finally, total personal income responses are displayed in Fig. 5. Across the census regions considered, the results indicate pronounced and rather persistent but increasingly smaller declines in income, consistent

[9]For a definition of the census regions see Appendix B. All state-level quantities are available from the authors upon request.

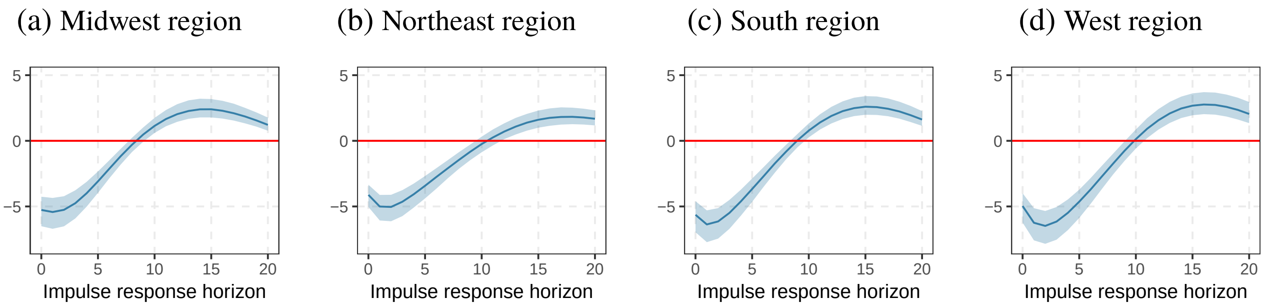

Fig. 4: Impulse response functions of employment in US states following a national uncertainty shock.
Notes: The solid blue line is the median response, the shaded blue area represents the 16th and 84th percentiles. The red line indicates the zero line. Results are based on 5,000 posterior draws. Sample period: 1985:Q1 – 2017:Q1. Front axis: quarters after impact.

with the aggregate decrease in real activity (see Fig. 2(b)), lead to weaker labor markets. While we can identify some minor differences in the shape and timing of the responses, regional differences appear to be somewhat muted.

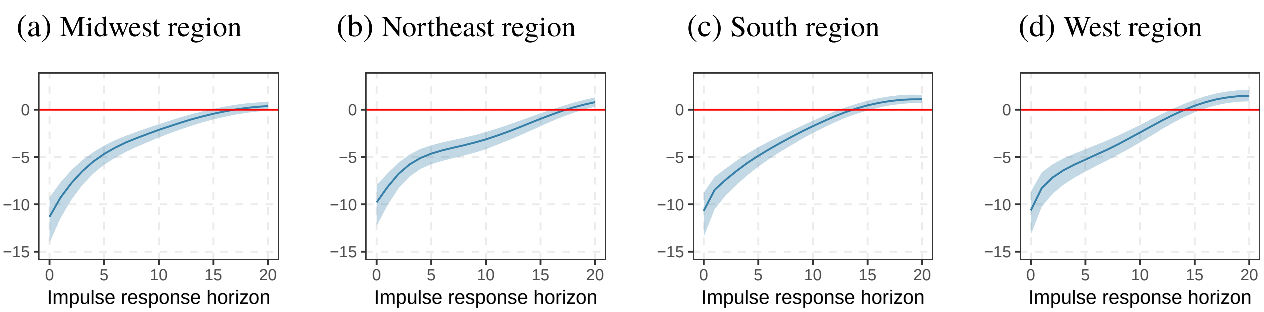

Fig. 5: Impulse response functions of total personal income in US states following a national uncertainty shock.
Notes: The solid blue line is the median response, the shaded blue area represents the 16th and 84th percentiles. The red line indicates the zero line. Results are based on 5,000 posterior draws. Sample period: 1985:Q1 – 2017:Q1. Front axis: quarters after impact.

To sum up, a national uncertainty shock yields reactions of real and financial quantities that are consistent with Bloom (2009), Jurado et al. (2015), Baker et al. (2016), Mumtaz and Theodoridis (2018), Carriero et al. (2018). When considering cross-regional variation in the impulse responses, little evidence of heterogeneity (in terms of the estimated impulse response functions) is evident. We conjecture that this may stem from the fact that our model assumes the autoregressive coefficients to originate from a common distribution, effectively introducing parameter homogeneity across regions when supported by the data.

4.2. *Impulse responses of income inequality*

To assess how a national uncertainty shock affects income inequality in the US, we first compute state-specific impulse responses, and average these to obtain responses at the level of the census regions for presentational purposes, and then consider boxplots of the posterior mean of state-level responses across the impulse response horizons to provide evidence on differentials between states and regions.

The regional impulse response functions of income inequality are presented in Fig. 6 that shows the posterior median along with the 16th and 84th percentiles of the posterior distribution of the responses of income inequality across the census regions. These responses reveal substantial heterogeneity, as opposed to the responses of the regional macroeconomic quantities described in Section 4.1. This heterogeneity is not only related to statistical significance but also to the shape and direction of the dynamic responses.

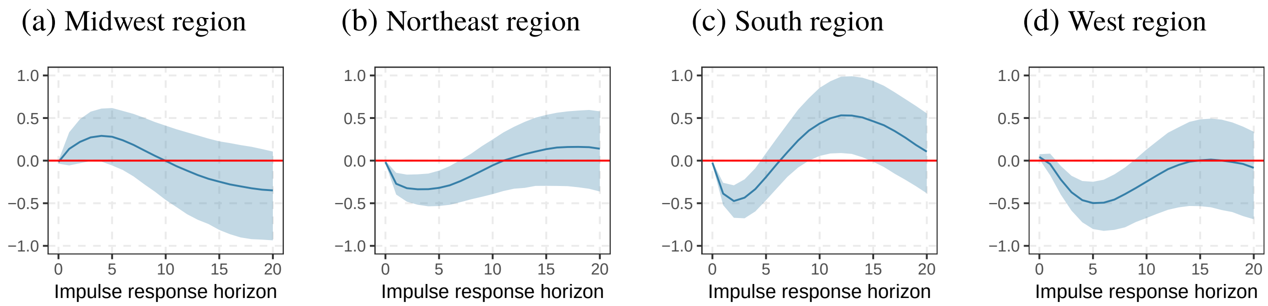

Fig. 6: Impulse response functions of household income inequality in US states following a national uncertainty shock.

Notes: The solid blue line is the median response, the shaded blue area represents the 16th and 84th percentiles. The red line indicates the zero line. Results are based on 5,000 posterior draws. Sample period: 1985:Q1 – 2017:Q1. Front axis: quarters after impact.

One common feature that all regions share is the slow reaction of income inequality to uncertainty. It is important to note that given our identification strategy, this slow reaction is not imposed a priori, but purely driven by the data. One potential interpretation is that the presence of wage and price rigidities translates into slower reactions of income inequality, with a potential delay of inequality responses that ranges from three (in case of the Northeast and South regions) to six quarters (in case of the Midwest).

The results for the Midwest (see Fig. 6(a)) are broadly consistent with recent evidence provided for the United Kingdom by Theophilopoulou (2018), who reports that inequality responses are positive in the short run, turning negative in the long run. Even though we do not observe a significant decline after about five quarters, there is some evidence that the initial increase in income inequality tends to fade out. In contrast, the inequality responses for the South (see Fig. 6(c)) indicate a decline over the first two quarters and a pronounced rebound after approximately ten quarters. The Northeast and West regions, shown in Figs. 6(b) and 6(d), also suggest that inequality falls in the short run but with less evidence in favor of a rebound after around 1.5 years.

If we consider the inequality responses in light of the reactions of the macroeconomic fundamentals described in Section 4.1, it is worth noting that regions displaying declining inequality levels are typically characterized by higher levels of capital income whereas the states located in the Midwest are generally accompanied by lower levels of capital and higher shares of labor income. This is broadly consistent with theoretical evidence provided in Kasa and Lei (2018), who show that wealthy agents invest a relatively high fraction of their wealth in risky assets. This strategy pays off during tranquil times, amplifying inequality, but tends to perform poorly in crisis episodes, effectively leading to a reduction in inequality.

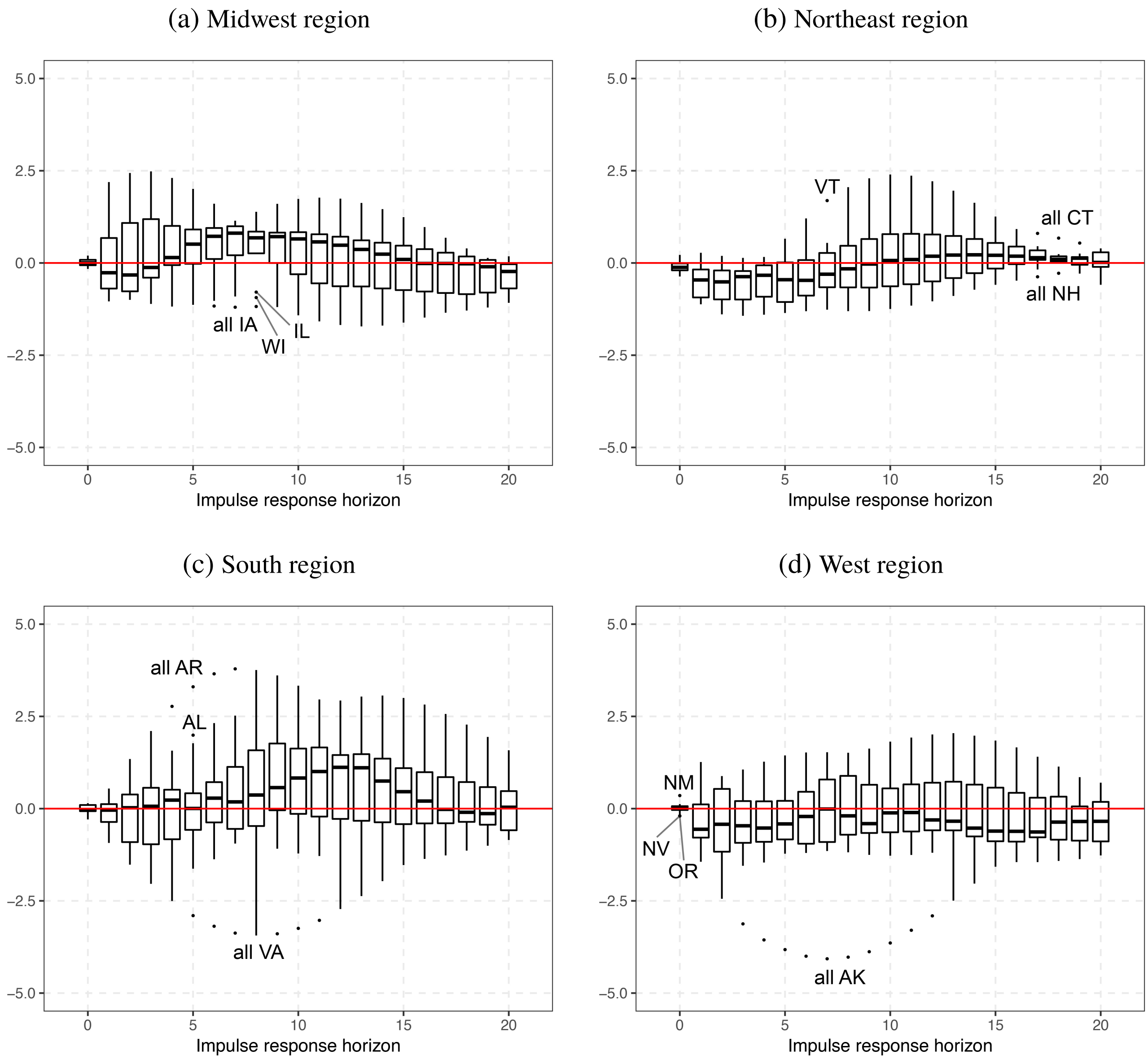

Fig. 7: Boxplot of median impulse response functions for household income inequality across states.
Notes: The red line indicates the zero line. Results are based on 5,000 posterior draws. Sample period: 1985:Q1 – 2017:Q1. Front axis: quarters after impact. For definition of the ISO-2 codes, see Appendix B.

Averaging state-level responses to the regional level may mask important intra-regional variation of inequality reactions. To provide some information on how much variation exists in the regions, Fig. 7 displays boxplots of the posterior mean responses for each state within a given region and across impulse response horizons. The spacing between the different parts of the boxes indicates the degree of cross-state dispersion in the posterior mean responses while black dots indicate outlying states.

The boxplots provide some interesting features. First, for the Northeast region (see Fig. 7(b)) we observe that if the reaction of income inequality (see Fig. 6(b)) is significant at a given time horizon, the corresponding cross-state dispersion tends to be small and centered below zero. This is especially true for short-term responses. Second, within-region variation in the South is evidently larger when compared to the others, especially for medium-term responses. This indicates elevated heterogeneity in terms of state-level responses within the region concerned. Third, for the South region, Virginia (VA) and Arkansas (AR) appear to be dominant outliers, both displaying stronger reactions on average. In the case of Arkansas, this implies more positive inequality responses while for Virginia, we observe income inequality responses that are more negative. Finally, within the West region, Alaska (AK) features outlying responses that point towards strongly decreasing levels of income inequality.

4.3. *The role of uncertainty shocks in explaining income inequality*

In this section, we asses the quantitative contribution of uncertainty shocks to movements in household income dispersion across regions. For this purpose, we consider the share of forecast error variance of income inequality explained by the uncertainty shock (see Fig. 8) as well as historical decompositions (see Fig. 9) that enable to shed light on the relevance of the uncertainty shock to explaining historical movements in income inequality.

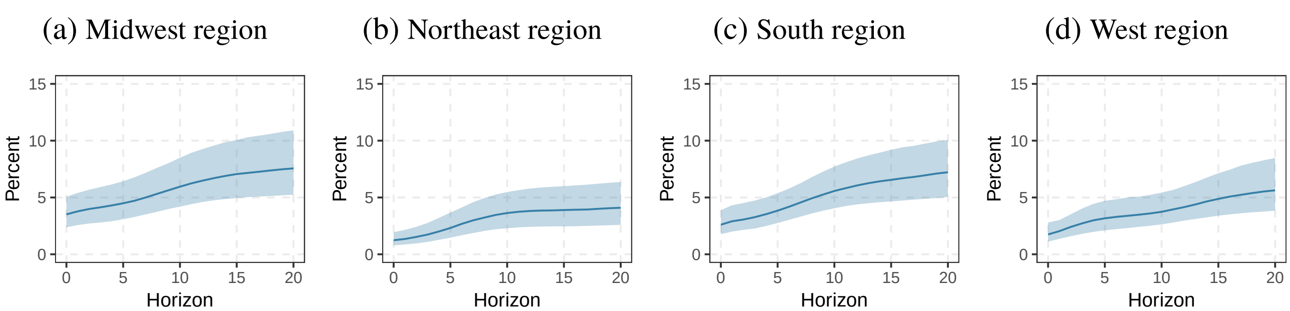

Fig. 8: Forecast error variance decompositions for income inequality in US census regions.
Notes: The solid blue line is the median response, the shaded blue area represents the 16th and 84th percentiles. The red line indicates the zero line. Results are based on 5,000 posterior draws. Sample period: 1985:Q1 – 2017:Q1. Front axis: quarters after impact.

Figure 8 displays forecast error variance decompositions for income inequality and indicates – consistent with Section 4.2 – pronounced differences across regions. We observe that the quantitative contribution of the uncertainty shock in explaining the forecast error variance of income inequality ranges from around two percent in the Northeast to about four percent in the Midwest, at the one-step-ahead horizon. This share rises considerably with the forecast horizon, peaking at approximately seven percent in the Midwest and South, while reaching roughly 3.5 percent in the Northeast. Notice that the share rises over time across all regions under consideration.

Figure 9 shows the contribution of the identified uncertainty shock over time and across regions. Several points are worth emphasizing. First, the quantitative relevance of the uncertainty shock is small

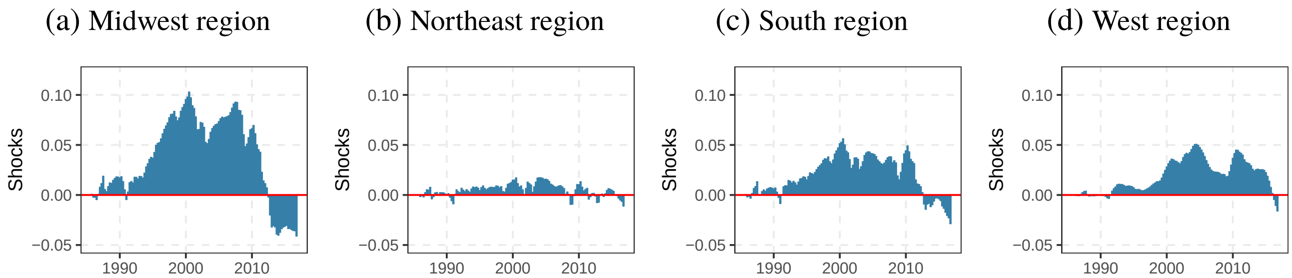

Fig. 9: Historical contributions of uncertainty shocks to income inequality.
Notes: The blue bars indicate the contributions of uncertainty shocks to the averaged inequality time series. The red line indicates the zero line. Results are based on the median of 5,000 posterior draws. Sample period: 1985:Q1 – 2017:Q1.

up to the beginning of the 1990s. This holds for all census regions. Second, for the Midwest and South, the contributions are positive up to 2011. From 2011 onwards, the contributions turn negative. Interestingly, this time span coincides with the period of the zero lower bound, indicating that there seems to be a relationship between the inequality-uncertainty nexus and unconventional monetary policy. Finally, the relative contributions strongly vary in size, with the importance of uncertainty shocks being highest in the Midwest and smallest in the Northeast.

4.4. *Explaining differences in inequality responses*

For explaining differences in state-level responses of income inequality, we conduct a regression analysis. As endogenous variable, we use the posterior median of the h-step ahead (for $h = 0, 4, 8, 12, 16$), cumulative, peak, minimum, and maximum responses. Specifically, the responses of income inequality for all states except the District of Columbia are regressed on a set of state-specific covariates averaged over time and weighted by the corresponding state-level gross regional product. While the approach suffers from issues like latent response variables, endogeneity, and potential model misspecification, it provides a rough gauge of the underlying trends in the data (see Kose et al., 2003, for a similar exercise using a dynamic factor model).

We choose nine explanatory variables that are potential determinants of income inequality. The first variable (*Higher Education*) relates to the proportion of citizens holding a bachelor's degree or higher and serves to establish the relationship between human capital and income inequality. Data is obtained from the US Census Bureau (Acemoglu, 1998; Autor et al., 2008). To control for differences in the exposure to international trade and globalization, we include data on the state-specific value of exports to all countries (Goldin and Katz, 2008) as the second explanatory variable (*International Trade*). Labor market institutions and the degree of unionization have also been identified as possible determinants of the distribution of income (Card et al., 2004). This is captured using information on the state-specific minimum wages per hour (*Minimum Wage*), and the union membership rate (*Union Membership*), defined as the percentage of wage and salary workers who are members of unions, taken from the Bureau of Labor Statistics.

There also exists a relationship between the sectoral composition of employment, economic development, and the income distribution (see Kuznets, 1955). To account for this, data on the share of workers employed in the manufacturing sector is included as an additional covariate (*Manufacturing*). Piketty and Saez (2003) provide evidence of profound changes in the composition of top incomes (relative positions between capital and wage income) and their surging importance (Piketty et al., 2018; Aghion et al., 2019). Correspondingly, data on the shares of income accruing to different parts of the income distribution across US states from the World Inequality Database (Alvaredo et al., 2018) are included (*Top One Percent* and *Top 10 Percent*). Furthermore, we calculate the share of wages and salaries proportional to total personal income (*Wage Share*). The set of explanatory variables is completed using data on the share of income related taxes to tax revenue in a state (*Income Taxation*), reflecting the relationship between the overall level of taxation and pre-tax income (Piketty et al., 2014).

Table 1 shows the regression results. Most variables included turn out to have no significant effect on income inequality reactions. In terms of significant effects, the sectoral allocation of employment within states, the composition of income in terms of labor and capital income, and different income groups exert some influence on inequality.

Starting with the share of employees in the manufacturing sector (*Manufacturing*), the results suggest that more employees in manufacturing are associated with lower impact responses. When we use this covariate to explain responses up to three-years-ahead, the coefficients change sign and point to a positive relationship between inequality and the share of workers in manufacturing. Turning to the share of wages and salaries in total personal income (*Wage Share*), the table shows that impact reactions tend to significantly rise with the wage share. The sign of the effect changes when longer-run reactions are considered, pointing towards a negative marginal relationship between the wage share and inequality reactions. When explaining the peak effect of the responses, the share of income related taxes proportional to overall tax revenues (*Income Taxation*) features a significantly negative regression coefficient. This suggests a negative relationship between a higher dependency on income taxes and peak reactions of inequality.

When considering the income composition and its potential effects of inequality responses, Tab. 1 highlights strong and significant effects associated with the income share covariates (*Top One Percent* and *Top 10 Percent*). For all endogenous variables considered, we find a negative relationship between the responses and the top one percent share. This pattern can be explained by noting that economic growth and productivity gains unequally benefit incomes, translating into stronger growth for high incomes. Since uncertainty shocks lead to a decline in real activity and adverse effects in financial markets, top incomes decline proportionally stronger and this leads to a decline in household inequality (Piketty et al., 2018).

By contrast, the positive relationship between the income share of the top 10 percent and responses of income inequality can be explained by the lower exposure of white collar professionals (e.g. lawyers, managers, and physicians) to weakening labor markets, when compared to blue collar workers. Increasing unemployment thus effectively weakens the bargaining position of blue collar workers, leading to wage cuts that strongly impact income inequality.

5. CLOSING REMARKS

This paper focuses on the relationship between macroeconomic uncertainty shocks and household income inequality using a novel large-scale econometric framework. Our model enables to assess how an unexpected increase in national uncertainty impacts the US economy at the state level, controlling for

Table 1: Explaining state-level impulse responses of income inequality.

	Impulse response								
	Impact	*Year 1*	*Year 2*	*Year 3*	*Year 4*	*Cumulative*	*Peak*	*Min.*	*Max.*
Intercept	-0.015^{***}	-0.072	-0.041	-0.033	-0.026	-0.961	-0.116	-0.042	-0.041
	(0.005)	(0.048)	(0.053)	(0.047)	(0.035)	(0.647)	(0.072)	(0.028)	(0.041)
Higher Education	0.001	-0.033	0.004	0.034	0.038	0.218	0.026	0.017	0.014
	(0.005)	(0.043)	(0.048)	(0.042)	(0.031)	(0.583)	(0.065)	(0.025)	(0.037)
International Trade	-0.002	-0.018	-0.012	-0.012	-0.012	-0.264	-0.027	-0.007	-0.016
	(0.002)	(0.015)	(0.017)	(0.014)	(0.011)	(0.200)	(0.022)	(0.009)	(0.013)
Union Membership	0.006	0.025	-0.043	-0.057	-0.027	-0.306	0.004	-0.003	0.004
	(0.004)	(0.035)	(0.039)	(0.034)	(0.025)	(0.471)	(0.053)	(0.020)	(0.030)
Minimum Wage	0.000	-0.001	0.001	0.001	0.000	0.003	0.000	0.000	0.000
	(0.001)	(0.001)	(0.001)	(0.001)	(0.001)	(0.016)	(0.002)	(0.001)	(0.001)
Income Taxation	0.001	-0.010	-0.014	-0.007	0.001	-0.116	-0.026^{*}	-0.003	-0.009
	(0.001)	(0.010)	(0.011)	(0.009)	(0.007)	(0.129)	(0.014)	(0.006)	(0.008)
Manufacturing	-0.024^{***}	0.113^{**}	0.165^{***}	0.058	-0.046	0.885	0.092	0.057^{*}	0.030
	(0.005)	(0.049)	(0.054)	(0.048)	(0.035)	(0.659)	(0.074)	(0.029)	(0.042)
Wage Share	0.011^{*}	0.080	-0.005	-0.066	-0.074^{*}	-0.213	-0.028	-0.008	-0.012
	(0.006)	(0.056)	(0.062)	(0.054)	(0.040)	(0.749)	(0.084)	(0.033)	(0.048)
Top One Percent	-0.075^{***}	-0.164	-0.159	-0.280^{*}	-0.279^{**}	-4.797^{**}	-0.661^{***}	-0.107	-0.316^{**}
	(0.016)	(0.144)	(0.160)	(0.140)	(0.104)	(1.939)	(0.216)	(0.084)	(0.123)
Top 10 Percent	0.057^{***}	0.136	0.140	0.252^{*}	0.260^{***}	4.280^{**}	0.552^{***}	0.110	0.251^{**}
	(0.014)	(0.130)	(0.143)	(0.126)	(0.093)	(1.741)	(0.194)	(0.076)	(0.111)
Observations	50	50	50	50	50	50	50	50	50
R^2	0.573	0.310	0.251	0.329	0.434	0.242	0.284	0.774	0.643
Adjusted R^2	0.467	0.137	0.064	0.161	0.292	0.053	0.104	0.718	0.554
Residual Error	0.605	5.531	6.115	5.357	3.970	74.246	8.283	3.231	4.719
F Statistic	5.373^{***}	1.793^{*}	1.342	1.960^{*}	3.067^{***}	1.280	1.583	13.703^{***}	7.199^{***}

Notes: The sample consists of all US states (except the District of Columbia due to data limitations). The dependent variable refers to the value of the impulse response function on impact, after one to four years, the cumulative impulse response function after 20 quarters, the level at the peak of the response, the minimum and the maximum response. Explanatory variables are the share of the population with a bachelor's degree or higher (*Higher Education*), the exposure to international trade measured using the value of exports (*International Trade*), union membership rates of the workforce (*Union Membership*), the minimum wage level (*Minimum Wage*), the share of income related taxes related to overall tax revenue (*Income Taxation*), the proportion of workers employed in the manufacturing sector (*Manufacturing*), the share of wages in total personal income (*Wage Share*), and the share of income accruing to the top 1 and top 10 percent of the income distribution (*Top One Percent* and *Top 10 Percent*), respectively. Standard errors in parentheses. Levels of significance: $^{*}p<0.1$; $^{**}p<0.05$; $^{***}p<0.01$.

potential spillovers between states. Moreover, to control for national movements in key macroeconomic aggregates, we include an additional VAR specification that is linked to the state models in a dynamic fashion.

The model is used to assess how national quantities react to movements in uncertainty, yielding results that are in line with the literature. Specifically, increases in uncertainty translate into a drop in real activity, prices, as well as interest rates. Consistent with the previous literature on uncertainty shocks, reactions of output provide considerable evidence in favor of a real activity overshoot. Regional reactions in unemployment, employment, and income confirm the findings based on national data, namely increases in unemployment, declines in employment, and a decrease in income. One key result is that differences across regions are small.

Reactions of income inequality to uncertainty shocks reveal that increases in uncertainty yield heterogeneous responses across space. Three out of the four census regions considered exhibit a negative reaction of the Gini coefficient while for the Midwest, we find that income inequality increases after around a year. This effect, however, fades out after a few quarters and eventually points towards decreasing levels of inequality, evidenced by significant posterior mass located below zero. For the South, the initial decline in income inequality is reversed after around ten quarters, with significant evidence for an increase in inequality in the medium term.

The quantitative contribution of the uncertainty shock in explaining income inequality is assessed by conducting a forecast error variance decomposition. The findings, again, point towards a large degree of heterogeneity across space. For some regions, uncertainty shocks play an important role in shaping income inequality dynamics whereas for others this role is somewhat smaller but still substantial. Historical decompositions enable us to investigate whether and when uncertainty shocks played a prominent role in determining income inequality over the estimation period.

We explain the state-specific impulse response functions for income inequality by a regression analysis featuring various quantities typically identified as drivers of income inequality. The results suggest that the reaction of household income inequality is affected by the composition of income and labor market fundamentals such as sectoral employment.

REFERENCES

Acemoglu D (1998) Why do new technologies complement skills? Directed technical change and wage inequality. *Quarterly Journal of Economics* 113(4), 1055–1089

Aghion P, Akcigit U, Bergeaud A, Blundell R and Hemous D (2019) Innovation and top income inequality. *Review of Economic Studies* 86(1), 1–45

Aguilar O and West M (2000) Bayesian dynamic factor models and portfolio allocation. *Journal of Business & Economic Statistics* 18(3), 338–357

Allenby GM, Arora N and Ginter JL (1998) On the heterogeneity of demand. *Journal of Marketing Research* 35(3), 384–389

Alvaredo F, Chancel L, Piketty T, Saez E and Zucman G (2018) World inequality database. URL: https:// wid.world/

Autor DH, Katz LF and Kearney MS (2008) Trends in US wage inequality: Revising the revisionists. *Review of Economics and Statistics* 90(2), 300–323

Baker SR, Bloom N and Davis SJ (2016) Measuring economic policy uncertainty. *Quarterly Journal of Economics* 131(4), 1593–1636

Basu S and Bundick B (2017) Uncertainty shocks in a model of effective demand. *Econometrica* 85(3), 937–958

Bloom N (2009) The impact of uncertainty shocks. *Econometrica* 77(3), 623–685

Caggiano G, Castelnuovo E and Groshenny N (2014) Uncertainty shocks and unemployment dynamics in US recessions. *Journal of Monetary Economics* 67, 78–92

Caldara D, Fuentes-Albero C, Gilchrist S and Zakrajšek E (2016) The macroeconomic impact of financial and uncertainty shocks. *European Economic Review* 88, 185–207

Card D, Lemieux T and Riddell WC (2004) Unions and wage inequality. *Journal of Labor Research* 25(4), 519–559

Carriero A, Clark TE and Marcellino M (2018) Measuring uncertainty and its impact on the economy. *Review of Economics and Statistics* 100(5), 799–815

Coibion O, Gorodnichenko Y, Kueng L and Silvia J (2017) Innocent bystanders? Monetary policy and inequality. *Journal of Monetary Economics* 88, 70–89

Cowell F and Flachaire E (2015) Statistical methods for distributional analysis. In Atkinson A and Bourguignon F, eds., *Handbook of Income Distribution*. Elsevier, Oxford, pp. 361–468
Crespo Cuaresma J, Feldkircher M and Huber F (2016) Forecasting with global vector autoregressive models: A Bayesian approach. *Journal of Applied Econometrics* 31(7), 1371–1391
Feldkircher M and Huber F (2016) The international transmission of US shocks–Evidence from Bayesian global vector autoregressions. *European Economic Review* 81, 167–188
Fernández-Villaverde J, Guerrón-Quintana P, Rubio-Ramírez JF and Uribe M (2011) Risk matters: The real effects of volatility shocks. *American Economic Review* 101(6), 2530–2561
Fischer MM and Wang J (2011) *Spatial Data Analysis: Models, Methods and Techniques*. Springer [Springer Briefs in Regional Science], Heidelberg
Flood S, King M, Ruggles S and Warren JR (2017) *Integrated public use microdata series, current population survey: Version 5.0 [dataset]*. IPUMS, University of Minnesota, Minneapolis
Gertler M and Karadi P (2015) Monetary policy surprises, credit costs, and economic activity. *American Economic Journal: Macroeconomics* 7(1), 44–76
Goldin C and Katz LF (2008) *The Race between Education and Technology*. Harvard University Press, Cambridge
Heathcote J, Perri F and Violante GL (2010) Unequal we stand: An empirical analysis of economic inequality in the United States, 1967–2006. *Review of Economic Dynamics* 13(1), 15–51
Huber F (2016) Density forecasting using Bayesian global vector autoregressions with stochastic volatility. *International Journal of Forecasting* 32(3), 818–837
Huber F, Fischer MM and Piribauer P (2017) The role of US-based FDI flows for global output dynamics. *Macroeconomic Dynamics* , first online published, doi:10.1017/S1365100517000086
Jarociński M (2010) Responses to monetary policy shocks in the east and the west of Europe: A comparison. *Journal of Applied Econometrics* 25(5), 833–868
Jurado K, Ludvigson SC and Ng S (2015) Measuring uncertainty. *American Economic Review* 105(3), 1177–1216
Kasa K and Lei X (2018) Risk, uncertainty, and the dynamics of inequality. *Journal of Monetary Economics* 94, 60–78
Kastner G (2016) Dealing with stochastic volatility in time series using the R package stochvol. *Journal of Statistical Software* 69(5), 1–30
Kastner G and Frühwirth-Schnatter S (2014) Ancillarity-sufficiency interweaving strategy (ASIS) for boosting MCMC estimation of stochastic volatility models. *Computational Statistics & Data Analysis* 76, 408–423
Koop G (2003) *Bayesian Econometrics*. Wiley & Sons, Chichester, UK
Kose MA, Otrok C and Whiteman CH (2003) International business cycles: World, region, and country-specific factors. *American Economic Review* 93(4), 1216–1239
Kuznets S (1955) Economic growth and income inequality. *American Economic Review* 45(1), 1–28
Leduc S and Liu Z (2016) Uncertainty shocks are aggregate demand shocks. *Journal of Monetary Economics* 82, 20–35
Lumley T (2004) Analysis of complex survey samples. *Journal of Statistical Software* 9(1), 1–19
Lumley T (2018) *Survey: Analysis of complex survey samples*. R-package version 3.34, URL: https://cran.r-project.org/web/packages/survey/
McCracken MW and Ng S (2016) FRED-MD: A monthly database for macroeconomic research. *Journal of Business & Economic Statistics* 34(4), 574–589
Meyer BD and Sullivan JX (2013) Consumption and income inequality and the great recession. *American Economic Review* 103(3), 178–83
Mumtaz H and Theodoridis K (2018) The changing transmission of uncertainty shocks in the US. *Journal of Business & Economic Statistics* 36(2), 239–252
Mumtaz H and Theophilopoulou A (2017) The impact of monetary policy on inequality in the UK. An empirical analysis. *European Economic Review* 98, 410–423
OECD (2011) *Divided We Stand – Why Inequality Keeps Rising*. OECD Publishing, Paris
Pesaran MH, Schuermann T and Weiner SM (2004) Modeling regional interdependencies using a global error-correcting macroeconometric model. *Journal of Business and Economic Statistics* 22(2), 129–162
Pessoa D, Damico A and Jacob G (2018) *Convey: Income concentration analysis with complex survey samples*. R-package version 0.2.1, URL: https://cran.r-project.org/web/packages/convey/

Petev I, Pistaferri L and Eksten IS (2011) Consumption and the Great Recession: An analysis of trends, perceptions, and distributional effects. In Grusky D, Western B and Wimer C, eds., *The Great Recession*. Russell Sage Foundation, New York, pp. 161–195

Piketty T and Saez E (2003) Income inequality in the United States, 1913-1998. *Quarterly Journal of Economics* 118(1), 1–41

Piketty T, Saez E and Stantcheva S (2014) Optimal taxation of top labor incomes: A tale of three elasticities. *American Economic Journal: Economic Policy* 6(1), 230–271

Piketty T, Saez E and Zucman G (2018) Distributional national accounts: Methods and estimates for the United States. *Quarterly Journal of Economics* 133(2), 553–609

Roine J, Vlachos J and Waldenström D (2009) The long-run determinants of inequality: What can we learn from top income data? *Journal of Public Economics* 93(7), 974–988

Spiegelhalter DJ, Best NG, Carlin BP and van der Linde A (2002) Bayesian measures of model complexity and fit. *Journal of the Royal Statistical Society: Series B* 64(4), 583–639

Stiglitz JE (2012) Macroeconomic fluctuations, inequality, and human development. *Journal of Human Development and Capabilities* 13(1), 31–58

Theophilopoulou A (2018) The impact of macroeconomic uncertainty on inequality: An empirical study for the UK. *MPRA Paper* 90448, University of Munich, Munich, URL: https://mpra.ub.uni–muenchen.de/90448/

van Treeck T (2014) Did inequality cause the U.S. financial crisis? *Journal of Economic Surveys* 28(3), 421–448

Verbeke G and Lesaffre E (1996) A linear mixed-effects model with heterogeneity in the random-effects population. *Journal of the American Statistical Association* 91(433), 217–221

Zellner A (1973) *An Introduction to Bayesian Inference in Econometrics*. Wiley & Sons, New York

A. FULL CONDITIONAL POSTERIOR SAMPLING

The prior setup described in Section 2 translates into a set of full conditional posterior distributions that have a well-known form. In what follows, we only briefly summarize the steps involved in obtaining a valid draw from the joint posterior distribution, and provide additional references that include more details on the exact posterior moments.

Our Gibbs sampler iterates between the following steps:

(i) The VAR coefficients in $\boldsymbol{\beta}_i$ can be sampled on an equation-by-equation basis, where conditional on $\boldsymbol{\Lambda f}_t$, the full conditional posterior distribution follows a Gaussian distribution with mean and variance taking a standard form (see, for instance, Zellner, 1973)

(ii) Using the fact that conditional on knowing $\{\boldsymbol{\beta}_i\}_{i=1}^N$ the conditional posterior of $\boldsymbol{\mu}$ does not depend on the data leads to a Gaussian full conditional posterior distribution that takes a well-known form (Koop, 2003).

(iii) The VAR coefficients for the national quantities $\boldsymbol{D}_p$ and $\boldsymbol{S}_q$ are sampled analogously to the state-specific parameters from multivariate Gaussian distributions on an equation-by-equation basis.

(iv) The free elements in $\boldsymbol{\Lambda}$ can, again, be simulated on an equation-by-equation basis. Notice that conditional on the latent factors, $\boldsymbol{\Lambda}$ is obtained by estimating a sequence of standard Bayesian regression models with heteroscedastic innovations (see Aguilar and West, 2000)

(v) For the latent factors $\{\boldsymbol{f}_t\}_{t=1}^T$, we simulate the full history by drawing from a set of independent Gaussian distributions,

$$\begin{aligned} \boldsymbol{f}_t|\bullet &\sim \mathcal{N}(\overline{\boldsymbol{f}}_t, \boldsymbol{P}_t) \\ \boldsymbol{P}_t &= \boldsymbol{H}_t - \boldsymbol{\Upsilon}_t\boldsymbol{\Theta}_t\boldsymbol{\Upsilon}_t' \\ \boldsymbol{\Upsilon}_t &= \boldsymbol{H}_t\boldsymbol{\Lambda}'\boldsymbol{\Theta}_t^{-1} \\ \overline{\boldsymbol{f}}_t &= \boldsymbol{\Upsilon}_t\boldsymbol{\varepsilon}_t. \end{aligned} \tag{A.1}$$

(vi) The full history of the log-volatilities is sampled using the algorithm outlined in Kastner and Frühwirth-Schnatter (2014); see also Kastner (2016).

We pick starting values for the parameters of the model and cycle through the algorithm described above for 50, 000 times, discarding the first 25, 000 draws as burn-in. For inference, we consider every fifth draw. It is worth mentioning that the employed algorithm exhibits excellent mixing and convergence properties.

B. DIVISION OF THE UNITED STATES INTO CENSUS REGIONS AND STATES

Table B: Census regions and US states.

Census Regions	**States**
Midwest	Illinois (IL), Indiana (IN), Iowa (IA), Kansas (KS), Michigan (MI), Minnesota (MN), Missouri (MO), Nebraska (NE), North Dakota (ND), Ohio (OH), South Dakota (SD), Wisconsin (WI)
Northeast	Connecticut (CT), Maine (ME), Massachusetts (MA), New Hampshire (NH), New Jersey (NJ), New York (NY), Pennsylvania (PA), Rhode Island (RI), Vermont (VT)
South	Alabama (AL), Arkansas (AR), Delaware (DE), District of Columbia (DC), Florida (FL), Kentucky (KY), Georgia (GA), Louisiana (LA), Maryland (MD), Mississippi (MS), North Carolina (NC), Oklahoma (OK), South Carolina (SC), Tennessee (TN), Texas (TX), Virginia (VA), West Virginia (WV)
West	Alaska (AK), Arizona (AZ), California (CA), Colorado (CO), Hawaii (HI), Idaho (ID), Montana (MT), Nevada (NV), New Mexico (NM), Oregon (OR), Utah (UT), Washington (WA), Wyoming (WY)

Notes: Abbreviations of states in parentheses.

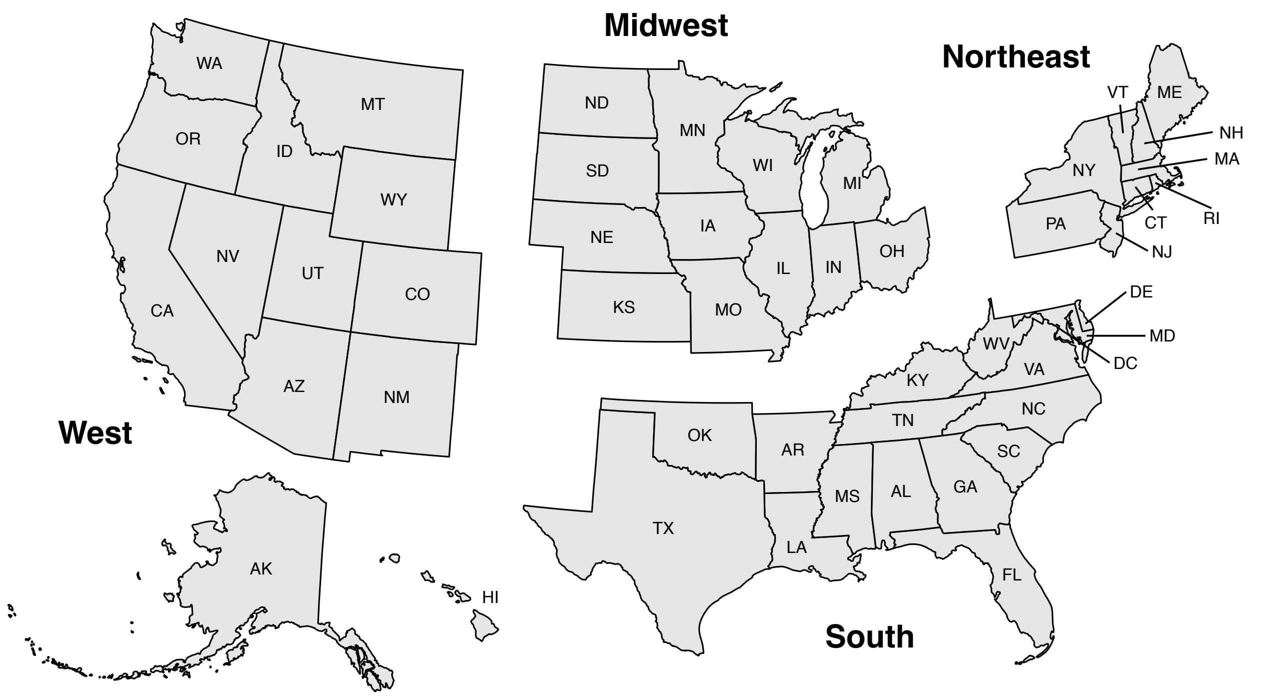

Fig. B: Map of the four census regions of the United States.